Electronic Supplementary Material (ESI) for Journal of Materials Chemistry
This journal is © The Royal Society of Chemistry 2012

Supporting information

High density Array of free standing Alumina Nanotubes Aligned Vertically on Substrates in a large area

By *Seung Yun Yang, Gumhye Jeon*, *and Jin Kon Kim*[*]

National Creative Research Initiative Center for Block Copolymer Self-Assembly,

Department of Chemical Engineering and Polymer Research Institute,

Pohang University of Science and Technology, Pohang, Kyungbuk 790-784, Korea

1. Fabrication of AAO membrane as an etching mask

Figure S1 shows a schematic for the fabrication of AAO mask on a polyimide (PI) film. First, the AAO mask was prepared by a two-step anodization process[1,2]. An Al sheet with a thickness of 1 mm (Goodfellow, 99.999%) was degreased with acetone, and electrochemically polished at 20V in ethanol/perchloric acid mixture (4:1 volume percent) at 7 ^{o}C. The polished Al sheet was first anodized in aqueous oxalic acid solutions of 0.3M for at 15 ^{o}C under 40V for 8 h. The top of the aluminum oxide showed poor ordering of pores, whereas the bottom side of the aluminum oxide had a good array of the pores. All of the first anodized alumina layers were completely removed by chromic acid (1.8 wt %) and phosphoric acid (6 wt %) aqueous solution at 65 ^{o}C for 6 h. After the aluminum oxide layer was removed, a well ordered dimple array was observed. Subsequently, a second anodization was carried out at the same condition employed in the first anodization step. After the second anodization, the pore size was controlled with immersion time into 0.1M phosphoric acid at

30 °C. Then, well-ordered and hexagonally packed pores were formed in AAO layer (Figure S1a). Thin AAO membrane with a thickness of ~ 600 nm was detached from the aluminum by a potential of 55 V in ethanol/perchloric acid mixture of 4:1 volume percent (Figure S1b) and directly floated on the PI film (Fig. S1c). Here, the AAO region which contacted the aluminum and had unopened (or incompletely formed) pores was placed on the air side. These unopened (or incompletely formed) pores of the AAO layer were removed by inductive coupled plasma etcher with CF_4 gas for 5 min (Fig. S1d). The adhesion between the AAO membrane and the PI film was good. The AAO membrane serves as an etching mask to prepare the cylindrical pores in the PI film. Figure S1e and f shows the top surface and cross-sectional view of the AAO membrane placed on the PI template, respectively. The AAO membrane has diameter of ~ 55nm and height of ~600nm.

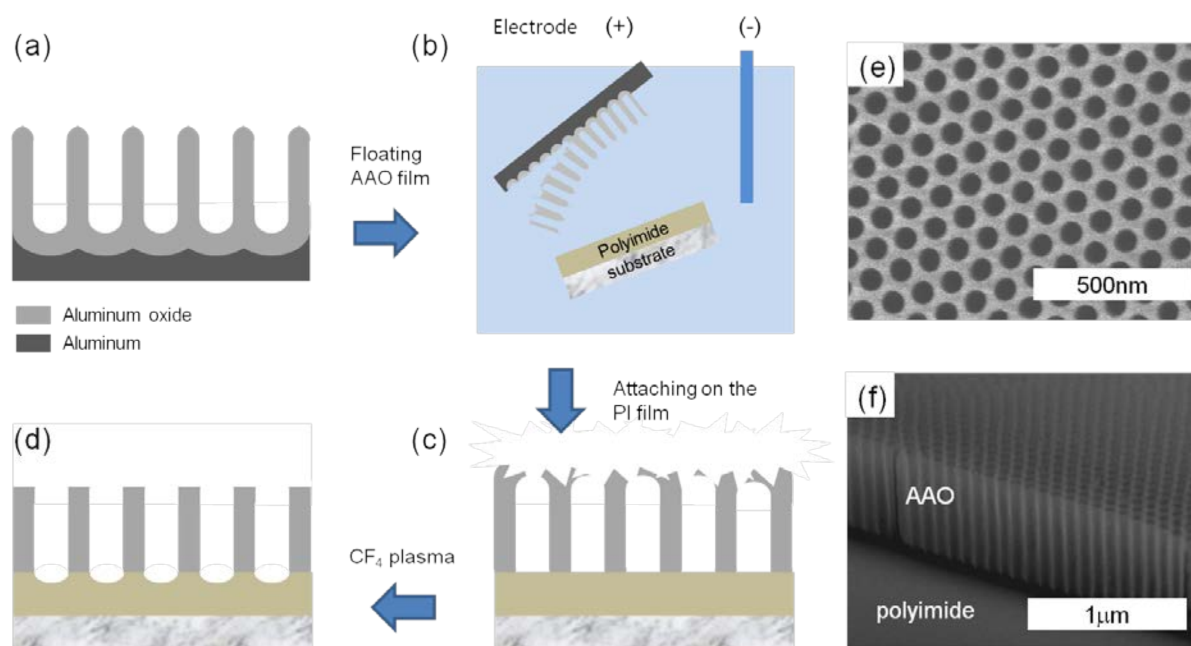

Figure S1. (a-d) Schematic for the fabrication of AAO mask onto PI thin film. (e, f) FE-SEM images showing the top and side view of AAO mask attached on the PI film.

2. Thermal stability of polyimide film

To evaluate thermal stability of polyimide (PI) film prepared by stepwise curing of amic acid, thermal gravimetric analysis (TGA) was performed using a Perkin Elmer TGA-7 by increasing the temperature from 30 to 600 °C at a heating rate of 10 °C/min under nitrogen atmosphere. As shown in Figure S2, PI film has a high thermal stability exhibiting a weight loss of less than 5% up to 500 °C. High thermal resistance of PI film could minimize the structural deformation of polymer template by heat, which could be generated by atomic layer deposition or etching processes.

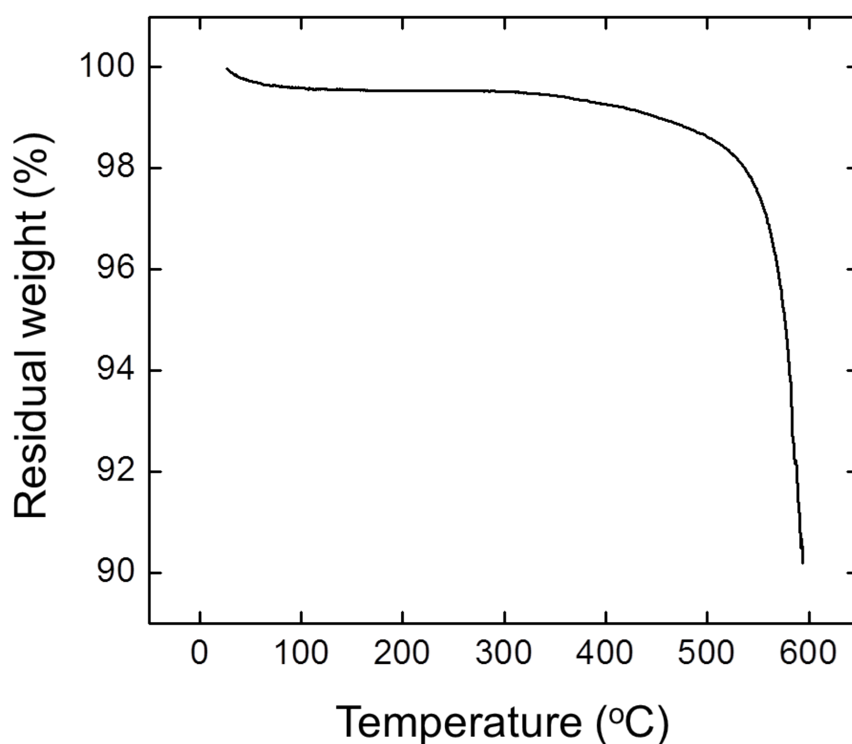

Figure S2. TGA curve of the PI film

This journal is © The Royal Society of Chemistry 2012

3. X-ray diffraction (XRD) of alumina nanotubes array on silicon substrate

ANTs array with a wall thickness of 10 nm was prepared using a polyimide template with a pore diameter of 70 nm, an interdistance of pores of 100 nm, and a thickness of 400 nm. After ALD of alumina was performed at 150 ^{o}C, the polyimide template was removed by CF_4 and O_2 plasma treatments. XRD pattern of this ANTs array was obtained with a Philips PW3710 diffractometer using CuKα radiation at 35 kV and 20 mA. As shown in Figure S3, as-prepared ANTs do not show any peak belonging to the crystalline structure of alumina in XRD pattern, suggesting that they are in amorphous state. This is because ALD of alumina was performed at lower temperature (150 ^{o}C).[3]

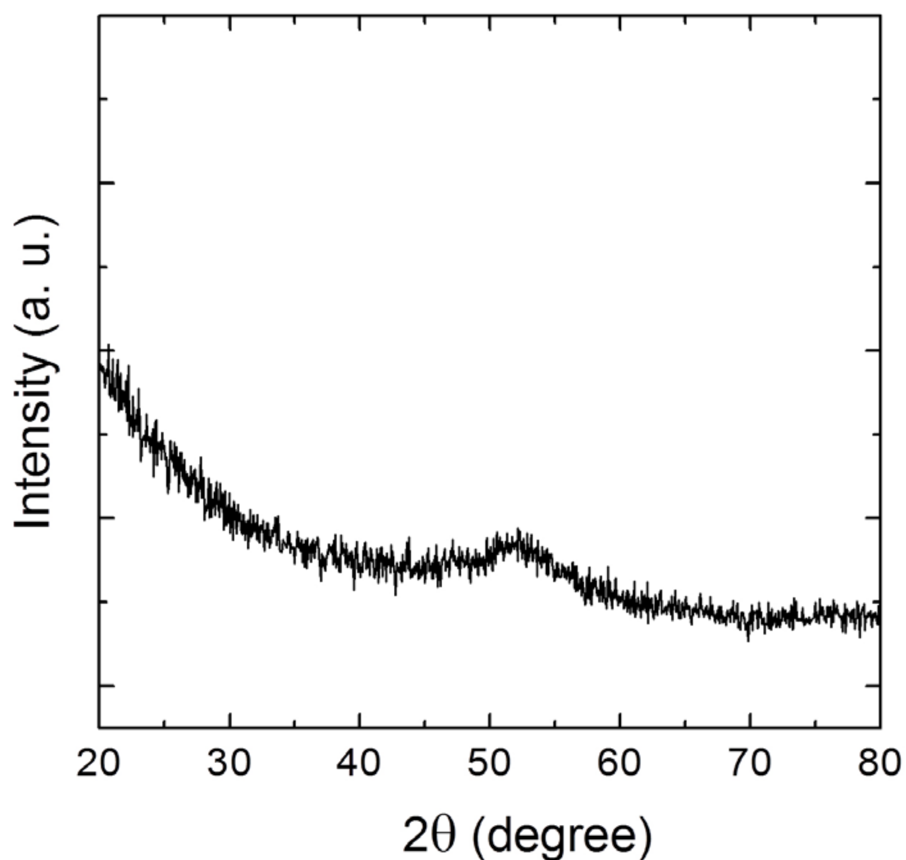

Figure S3. XRD pattern of the alumina nanotubes (ANTs) on a silicon substrate.

4. Control of pore size and height in the nanoporous PI templates

Figure S4(a-c) gives top and cross-sectional FE-SEM images for nanoporous PI templates with different pore sizes. The nanoporous PI templates with pore sizes of 15 nm, 40 nm and 75 nm were fabricated by O_2 plasma etching with the aid of AAO masks having pore diameters of 15 nm, 40 nm and 60 nm, respectively (Figure S4a-c). Although pore widening was observed especially for larger pores and thicker films (larger than 1 μm), a PI film with a thickness up to 2 μm was fully etched and excellent long range ordering of the pores was obtained (Figure S4d).

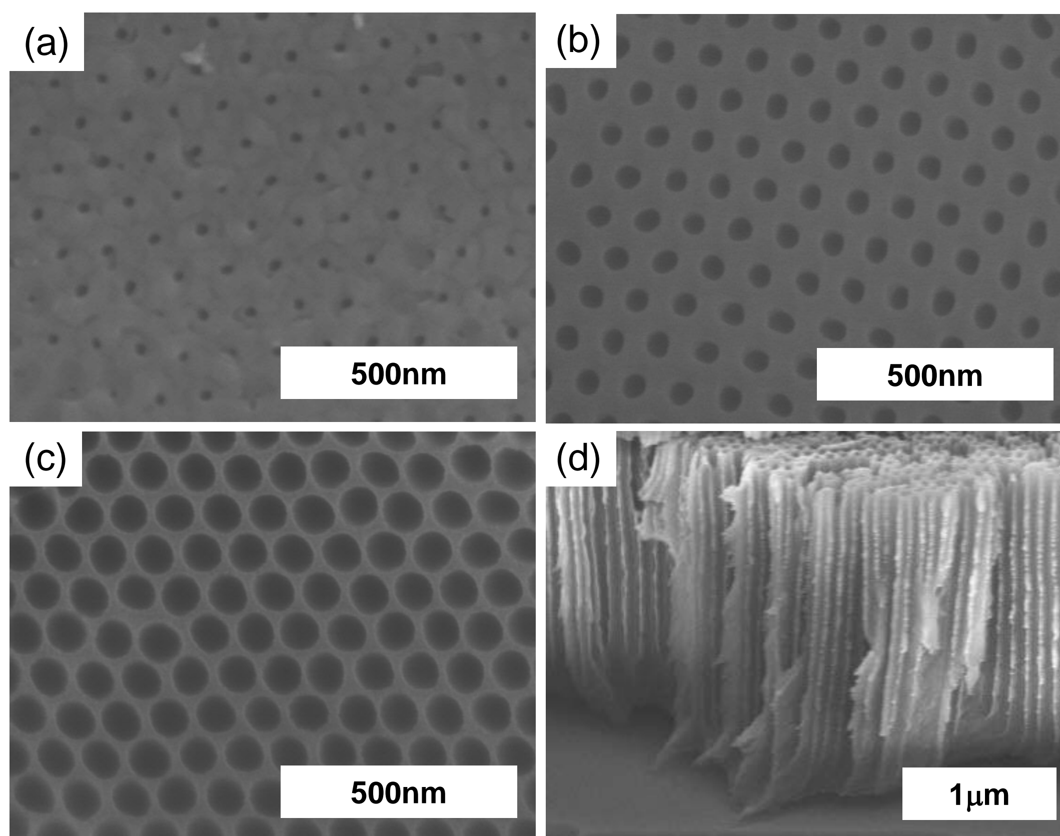

Figure S4. Various pore diameters ((a) 15nm, (b) 40nm and (c) 75 nm) in the nanoporous PI templates fabricated from different pore sizes of the AAO etching mask. (d) Cross-sectional image of the nanoporous PI template with a diameter of 75 nm. PI template with a thickness up to 2 μm was fully etched and pores touched the substrate surface.

5. The effect of chemical structure of the polymer on O_2 plasma etching

To compare the etching rate of polymers depending on their molecular structures to oxygen plasma, we performed the pattern transfer to polystyrene (PS) and polyimide (PI) films with AAO mask. The film thickness for both is 2.5 μm. O_2 plasma was performed at a flow of 5 sccm, a working pressure of 5 mTorr and the chuck power of 300 W for 35 min. Hole patterns in the AAO mask were transferred up to ~ 500 nm from the top surface of the PS film, but it could not be fully etched throughout the entire film thickness (2.5 μm) even at a long oxygen plasma etching (1 h). However, nanoholes in the PI template span throughout the entire film thickness. This effective etching by oxygen plasma is caused by the presence of oxygen atoms in PI, which act as a cleavage site during oxygen plasma etching.

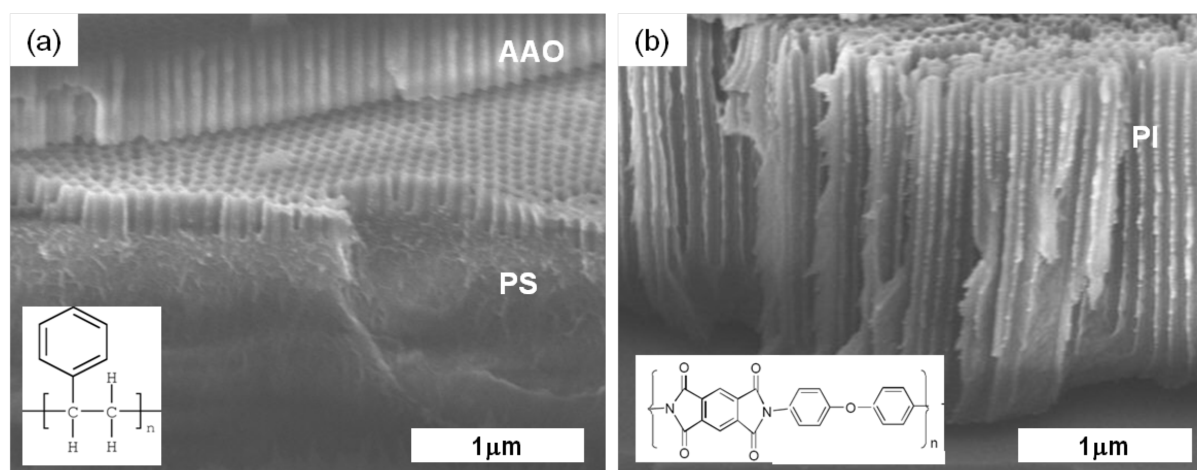

Figure S5. Cross-sectional SEM images of (a) PS and (b) Polyimide film after O_2 plasma etching. Inset shows the chemical structure (repeating unit) of the polymers.

6. High density array of alumina nanotubes on various substrates in a large area

Since PI film was made from spin-coating of amic acid followed by stepwise curing, it can be prepared on various solid substrates. As shown in Figure S6a, nanoporous PI templates with a thickness of 400 nm were prepared on the platinum-coated silicon wafer, ITO glass, a silicon wafer with natural oxide having a thickness of 3 nm, and the polymer film (Kapton®, DuPont). In case of the polymer substrate, to avoid etching of the underlying polymer film, an Au layer of ~ 50 nm, which acts as an etching stop layer, was deposited on a polymer substrate before PI film coating. The AAO mask was easily peeled off after O_2 plasma etching by using 3M Scotch Tape (Figure S6b). After alumina ALD and the sequential plasma treatments for removal of the top alumina layer and the PI template, high density array of ANTs with an excellent long lateral ordering was prepared in a large area (inch scale) (Figure S6c).

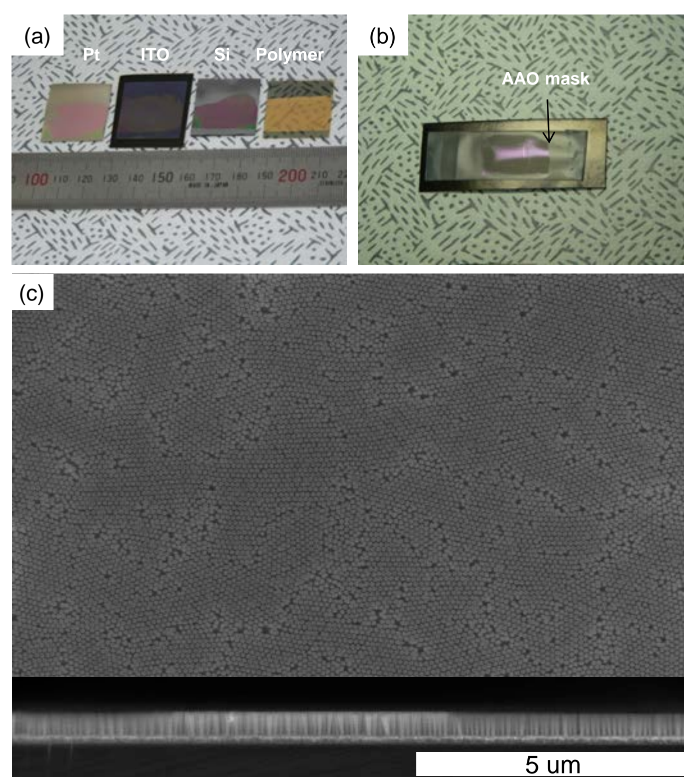

Figure S6. (a) PI templates prepared on various substrates, (b) Detached AAO mask after O_2 plasma using Scotch Tape, and (c) SEM images (top and cross sectional images) showing a high density array of ANTs with an excellent long lateral ordering in a large area.

7. Characterization of ANTs layer by characteristic matrix theory (CMT)

The porosity (f_{pore}) of a layer with a high density array of ANTs at a given wall thickness is calculated by (see Figure S7)

$$f_{pore} = 1 - \frac{(\pi/4)\left(d^2 - (d-2w)^2\right)/2}{\left(\sqrt{3}/4\right)L^2} = 1 - \frac{2\pi w(d-w)}{\sqrt{3}L^2} \quad \text{(S1)}$$

Here, d, L, and w are the outer diameter of ANT (70 nm) and the center to center distance between neighboring ANTs (100 nm), and the wall thickness. For w = 15 nm, the porosity is calculated to be 0.70.

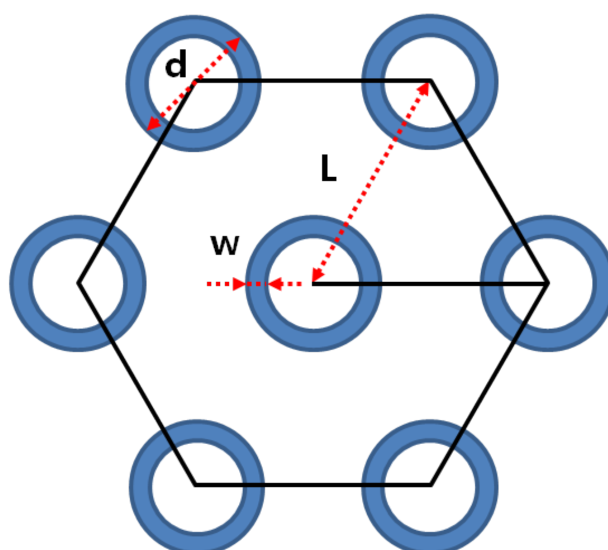

Figure S7. Calculation of porosity at a high density array of hexagonally packed ANTs.

The refractive index and thickness of the ANTs layer on a glass were fitted by one layer model of characteristic matrix theory[4,5] and the results are shown in Table S1. The fitted thickness of ANTs layer is well matched with the length of ANTs (~110nm) observed in SEM images (Figure 4g-i). Once the predicted n is given, the wall thickness of ANTs is also predicted by eq (1) in the text and eq (S1) and given in Table S1. These values were well matched with the deposition thickness of alumina by ALD.

Table S1. Predicted refractive index and dimensions of ANTs layer.

Wall thickness of ANTs (nm)	Predicted refractive index (n)	Predicted thickness(nm)	Predicted wall thickness (nm)[a]
6	1.12	105	6.3
10	1.19	102	10.5
15	1.25	108	16.1

[a] Assume that the ANTs have the outer diameter of 70 nm, and the center to center distance between neighboring ANTs of 100 nm.

Figure S8 gives the predicted reflectance of ANTs with various wall thicknesses by using CMT. Due to the outer diameter of ANTs was 70 nm, ANTs becomes alumina nanopillars at a wall thickness of 35 nm. It is clearly shown that when the wall thickness of ANTs is either smaller or larger than 15 nm, the zero reflectance could not be achieved. This indicates that the array of alumina nanotubes with a wall thickness of ~ 15 nm gives the best AR.

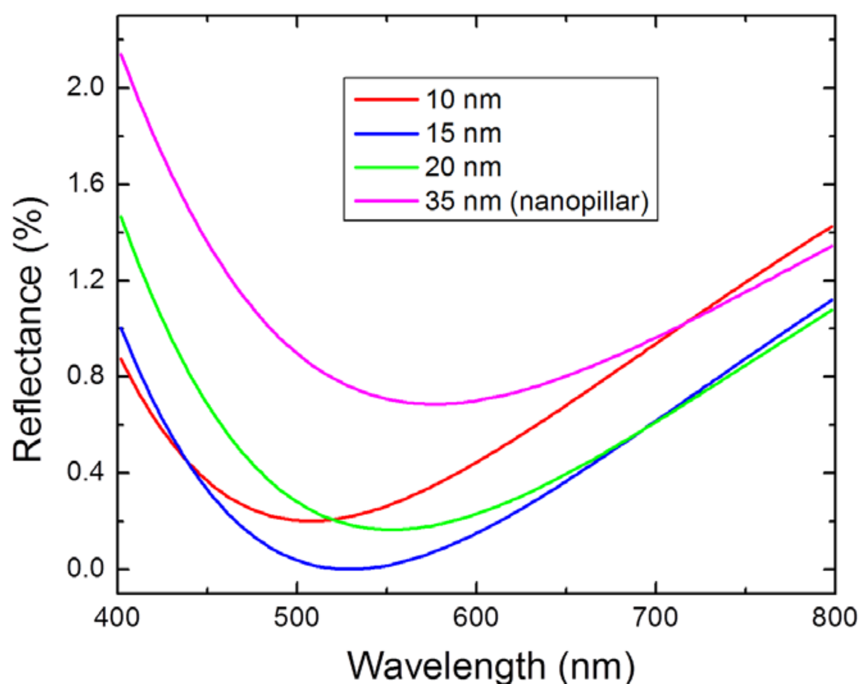

Figure S8. Predicted reflectance curves for the array of ANTs with different wall thicknesses.

This journal is © The Royal Society of Chemistry 2012

References

[1] A. P. Li, F. Müller, A. Birner, K. Nielsch, U. Gösele, *Adv. Mater.* 1999, 11, 483.

[2] G. Jeon, S. Y. Yang, J. Byun, J. K. Kim, *Nano Lett.* 2011, 11, 1284.

[3] G. Krautheim, T. Hecht, S. Jakschik, U. Schröder, W. Zahn, Appl. Surf. Sci., 2005, 252, 200.

[4] H. A. Macleod, *Thin-film optical filters*, Adam Hilger, London, UK 1986.

[5] M. S. Park, Y. Lee, J. K. Kim, *Chem. Mater.* 2005, 17, 3944.